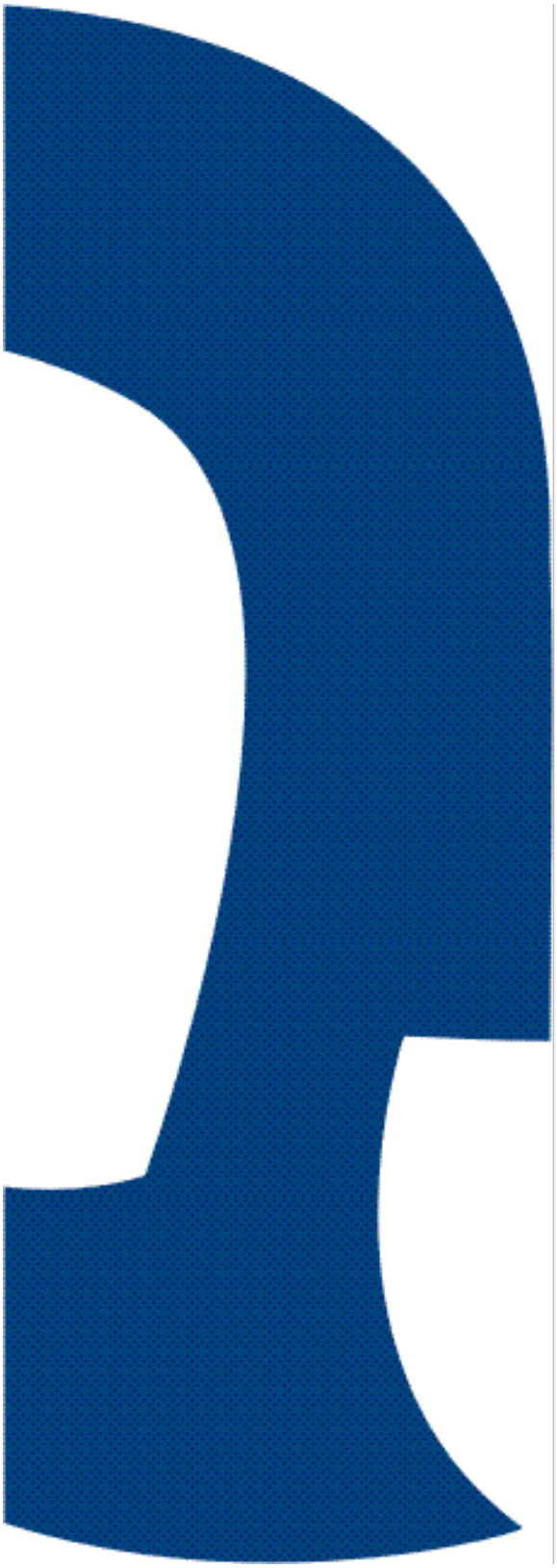

VARIABILITY OF THE WATER MASSES IN THE NORTH ATLANTIC SUBRTROPICAL GYRE

Laura Domènech Segú

Curso 2021/2022

Mentors

Dra. María Dolores Pérez-Hernández

Dr. Alonso Hernández-Guerra

Trabajo de Fin de Título para la obtención del título del Grado en Ciencias del Mar

Index

1. INTRODUCTION **5**

2. DATA AND METHODS **7**

3. WATER MASSES **10**

4. RESULTS **11**

4.1 TRANSOCEANIC Θ/S ISOBARIC CHANGES 11
4.2 Θ/S ISOBARIC CHANGES AT THE EASTERN BOUNDARY OF THE NASG 14
4.3 BINDOFF AND MCDOUGALL (1994) DECOMPOSITION AT THE A05 TRANSOCEANIC SECTION 18
4.4 BINDOFF AND MCDOUGALL (1994) DECOMPOSITION AT THE EASTERN BOUNDARY OF THE NASG 20

5. DISCUSSION **22**

6. CONCLUSION **25**

7. BIBLIOGRAPHY **26**

Abstract

At 24.5ºN the global heat transport is maximum, and most of this transport is due to the Atlantic Ocean. Changes in the oceanic heat transport can be related to changes in the water masses properties. This study focuses in understanding long term-changes and interannual variability of water masses properties in this latitude embedded on the North Atlantic Subtropical Gyre (NASG). Firstly, three hydrographic cruises at the 24.5ºN section carried out in 1981, 1998 and 2015 are selected to understand the full basin water masses changes of the NASG. Secondly, a deeper study focussing on the eastern boundary of the NASG is done. For this purpose, the eastern side of the 24.5ºN section is used together with four high-resolution hydrographic cruises carried out in 1997, 2007, 2014 and 2017 north of the Canary Islands (29ºN). The Bindoff & McDougall (1994) analysis is done to identify whether the observed changes are due to a vertical displacement of isoneutrals or due to changes along isoneutrals (differences in water properties). The results show a continuous warming and salinity increase of the NACW from 1957 to 2015 (0.1°C decade^{-1} and 0.01 decade^{-1} respectively) that comes with a temperature-diven deepening of the layer. At the Eastern boundary this trend higher but also consistent between 1997 and 2017. A 0.1°C decade^{-1} warming is also observed in IW from 1957 to 2004. Trends in the Canary area have been more difficult to infer due to high seasonality and the presence of mesoscale processes. Nevertheless, a decrease on the Mediterranean Water properties is observed for nearly two decades. For both A05 and Eastern Boundary sections, we find a weak cooling and freshening in the deep waters.

Key words: Atlantic Ocean, isobaric changes, isoneutral displacements, water masses properties, Canary Basin, eastern boundary, Interannual variability, North Atlantic Subtropical Gyre

1. Introduction

The North Atlantic Subtropical Gyre (NASG) constitutes a large hydrographic component of the North Atlantic Ocean. The NASG is wind-driven and, due to its tight relationship with the atmosphere, reacts very sensitively to climatic changes (Reißig et al., 2019). The 24.5ºN hydrographic section lies in the middle of the NASG. In this latitude, the global heat transport is maximum, and the main contributor to this transport is the Atlantic Ocean (Trenberth & Caron, 2001). Hence, changes in water masses or changes in the water masses characteristics at 24.5ºN can lead to changes in the global climate. The 24.5ºN section has been studied since 1957 (Bryden et al., 1996; Fuglister, 1960; Hernández-Guerra et al., 2014; Parrilla et al., 1994; Roemmich & Wunsch, 1985)

Though most of the studies cited above have focused in transport and on its contribution to the Atlantic Meridional Circulation (AMOC), some have reported interannual temperature and salinity changes. Parrilla et al., (1994) found that the water masses extending between 800-2500 m depth have warmed 0.32ºC over the 1957-1992 period (0.09ºC decade^{-1}), with a maximum of 0.1ºC decade^{-1} at 1100 m. This increasing trend persisted until 2004, being of 0.098ºC decade^{-1} for the layer between 200 and 2500 dbar (Cunningham & Alderson, 2007). Cunningham & Alderson (2007) also mentioned that the western side of the basin dominates the full-basin changes for the 1957-2004 period. However, Vargas-Yáñez et al., (2004) encountered that for the 1992-2002 period, the eastern basin had warmed at a rate of 0.25ºC decade^{-1}, being this rate higher than that of the west side. In contrast, Vélez-Belchí et al., (2010) reported a cooling of -0.19ºC decade^{-1} for the water masses shallower than 2000 dbar, and a maximum freshening of -0.05 decade^{-1} at 800 dbar for the 1998-2006 period. These authors also found that Deep Waters presented a freshening and cooling from 1957 to 2006. Parrilla et al., (1994) found that this cooling is an order of magnitude less than the warming observed in the upper layers, and that the maximum rate occurs at 3750 m depth (-0.009ºC decade^{-1}). Vargas-Yáñez et al., (2004) pointed out that, for the 1992-2002 period, changes in the layer among 350-1000 dbar can be associated to a deepening of isopycnals in order to maintain the θ/S relationship. On the other hand, in the first 350 dbar, changes can be split into cooling along isoneutrals and warming due to the deepening of the neutral surfaces. Cunningham & Alderson, (2007) also identified the deepening of isoneutrals as the main reason for the warming seen from 1951 to 2004, finding the highest increase between 1992-1998 interval (Vélez-Belchí et al., 2010).

The seasonal cycle of the eastern boundary of the NASG plays a major role in the seasonality of the AMOC (Pérez-Hernández et al., 2015; Vélez-Belchí et al., 2017). Chidichimo et al., (2010) studied the first three and a half years of RAPID-MOCHA data, finding an AMOC peak-to-peak seasonal cycle of 6.7 Sv, and attributing 5.2 Sv to the eastern boundary. These results were corroborated by Kanzow et al., (2010). This author

also pointed out that the seasonal variability of the upper-mid ocean may be attributed to changes in the eastern boundary stratification. Therefore, it is important to study how water masses change at the eastern boundary in order to fully understand basin-wide changes on the NASG and AMOC.

Long-time trends in temperature and salinity at the eastern boundary were firstly studied by Benítez-Barrios et al., (2008). They observed warming and salinification of the North Atlantic Central Water (NACW; from 100 to 350 dbar) with a temperature and salinity maximum of 1.92ºC and 0.46 from 1997 to 2006 (2.13ºC decade^{-1} and 0.51 decade^{-1} respectively). Slightly deeper in the water column, a freshening, occurring without changes in temperature until 600 dbar was also reported. Benítez-Barrios et al., (2008) determined that these changes are due to a deepening of the neutral surfaces but can offset the changes along isoneutrals. In addition, these authors estimated a warming and increasing salinity trend from 1500 dbar to 2300 dbar of 0.29ºC and 0.0475 decade^{-1}, respectively. In this case, deepening of isoneutrals was the main cause of this warming. Expanding the time coverage, Vélez-Belchí et al., (2015) studied the temperature and salinity trends from 1982 to 2013, finding a mean warming of 0.28ºC decade^{-1}. They estimated a warming of 0.20ºC decade^{-1} in NACW (200-600 dbar) with an increase of salinity around 0.03 decade^{-1}. This warming occurs due to the deepening of neutral surfaces (Vélez-Belchí et al., 2015). The warming seen by Benítez-Barrios et al., (2008) in North Atlantic Deep Water (NADW) is also observed in Vélez-Belchí et al., (2015). Meanwhile, from 2600 dbar to bottom a cooling (-0.01ºC decade^{-1}) and a freshening (-0.002 decade^{-1}), produced by the freshening of the sub-polar North Atlantic since 1970, is reported in Curry & Mauritzen, (2005).

The eastern boundary of the NASG presents a high seasonal variability in the upper and intermediate levels (Machín et al., 2010). In the upper layers, the Canary Current recirculates surface waters between the Azores Current and the North Equatorial current. This current shifts towards the African coast during summer and towards the western islands of the Canary archipelago in winter (Casanova-Masjoan et al., 2020; Machín et al., 2010; Stramma & Siedler, 1988). Also, at the surface layer, there is variability due to the nearby African upwelling that provides with surface cold water and generates an elevation of the isoneutrals in the eastern boundary. Though the upwelling takes place throughout the year, it is stronger in the spring and summer months (Navarro-Pérez & Barton, 2001). At intermediate layers, the seasonal variability of the eastern boundary resides on the seasonal cycle of the poleward undercurrent (Vélez-Belchí et al., 2017). In this layer, Mediterranean Water (MW) and Antarctic Intermediate Water (AAIW) coexist. MW predominates around the western islands, mainly due to the presence of Meddies while AAIW is found constrained to the Lanzarote Passage (LP) during fall (Hernández-Guerra et al., 2017; Vélez-Belchí et al., 2017).

In this study, section 24.5ºN is chosen as a representation of the NASG due to its relevance for the global heat transport. In addition, a detailed study of the eastern boundary of the NASG is carried out using data obtained from hydrographic cruises carried out north and south of the Canary Islands. The aim is to study the variability of potential temperature and salinity at 24.5ºN from 1981 to 2015 and to further explore the trends seen so far by other authors. The variability and trends in the eastern boundary will also be studied to see if they are reflected throughout the eastern Atlantic Ocean basin. To achieve this purpose the sections have been structured as it follows: in section 2 data and methodology applied are described. After describing the different Water Masses that can be found in the 24.5ºN and Canary region in section 3, section 4 presents the results obtained when applying the methodology, first, isobaric changes are explained (section 4.1), followed by their isobaric change decomposition in section 4.2; in section 5 results are discussed and in section 6 conclusions are presented.

2. Data and Methods

To study the NASG three different transatlantic cruises from the World Ocean Circulation Experiment (WOCE) and, later, Global Ocean Ship-based Hydrographic Investigations Program (GO-SHIP) programs are used. These programs pursued to improve the ocean models to predict decadal climate variability and change, (McNichol et al., 2000) and to provide with a dataset with decadal resolution to study changes in heat, freshwater, oxygen, and other relevant ocean properties. Here we will use full-depth vertical profiles of potential temperature and salinity from the A05 section, done at 24.5ºN. Years 1981, 1998, and 2015 (Table 1) are selected to study interannual variations of the NASG (Figure 1a). The stations corresponding to the Florida longitudes are not used, since they were only sampled in 1981, so a comparison could not be made.

Table 1. Start and end date for the different hydrographic cruises.

Section	Cruise Name	Year	Dates
24.5ºN - A05		1981	11 August - 4 September
		1998	23 January -22 February
		2015	7 December -18 January
29.2ºN	Meteor 37	1997	7-20 January
	RaProCan0207	2007	16-21 February
	RaProCan1410	2014	14-17 October
	RaProCan1704	2017	20-30 April

A detailed study of the eastern boundary is carried out with the easternmost stations of the A05 sections (Figure 1b) and four local high-resolution cruises (**Error! Reference source not found.** 1). During the CANIGO (Canary Islands Azores Gibraltar Observations) project, a box-like section around Canary Islands was done on a seasonal basis during 1990's. The purpose was to gain a better understanding of the physics, biogeochemistry, and paleo-oceanography of the eastern subtropical North Atlantic (Parrilla et al., 2002). In later years, the *Radial Profunda de Canarias* (RaProCan) project, which is the Canary Islands component of the Spanish Institute of Oceanography (IEO) ocean observing system (Tel et al., 2016; Vélez-Belchí et al., 2015), monitors the Canary basin with sections repeatedly done once or twice a year since 1997. For this study, we selected the CANIGO cruise done in 1997 and the RaProCan 2007, 2014, and 2017 cruises (Table1**Error! Reference source not found.**). For each cruise, 16 common stations are selected (Figure 2).

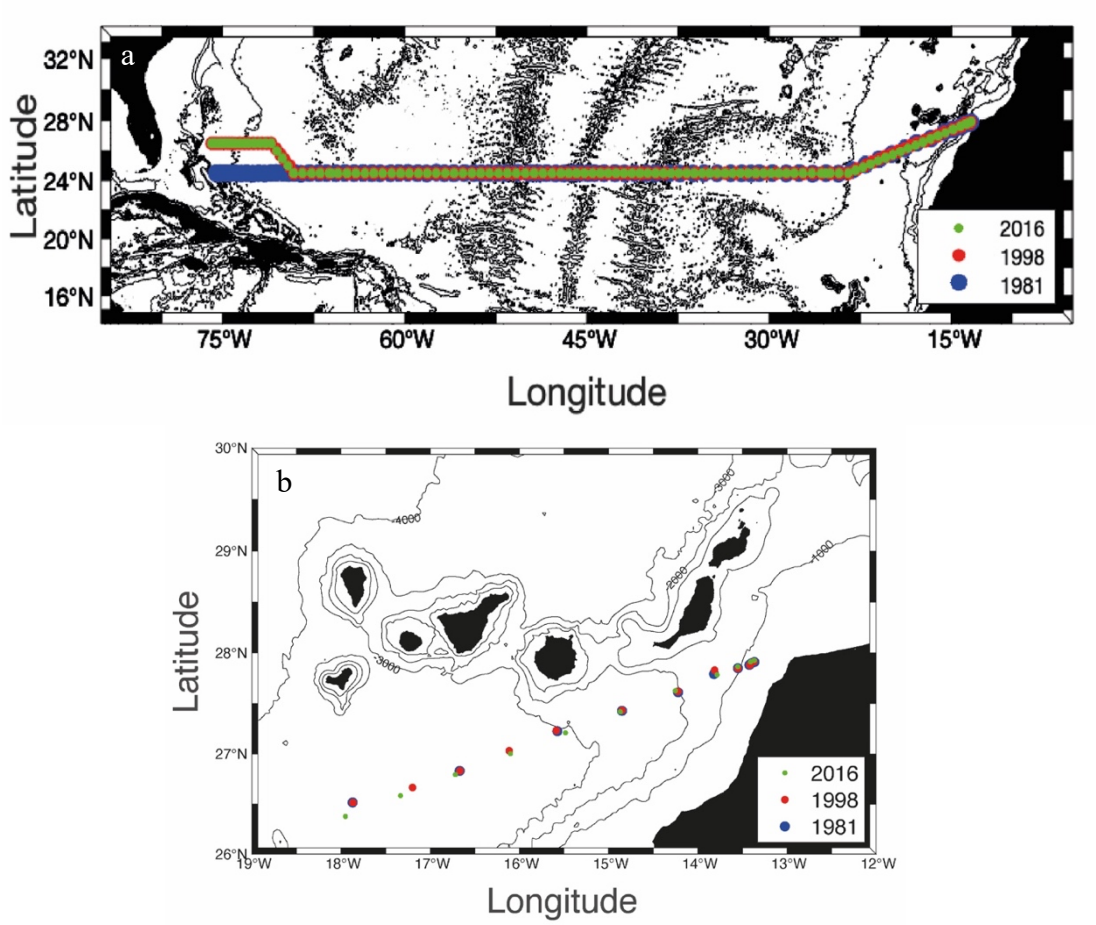

Figure 1. (a) WOCE A05 hydrographic stations carried out in 1981, 1998 and 2015 and (b) eastern boundary zoom of the same cruises.

A rosette unit, equipped with a Seabird911+ CTD (Conductivity Temperature Depth) sensor was used to obtain full-depth profiles of salinity and temperature every 2 dbar in all the years. The temperature sensor has an accuracy/stability of ±0.004ºC. Salinity water samples were analyzed on a Guideline AUTOSAL Model 8400B to get an accuracy of

0.003. Due to the different sampling schemes between the three A05 transatlantic sections, it is necessary to interpolate the different variables (potential temperature, salinity, and neutral density) to a regular grid of coordinates and pressure. A Laplacian-spline interpolation is used to create regular matrices of the different oceanic variables with a grid spacing of 0.5º in longitude and of 40 dbar in pressure.

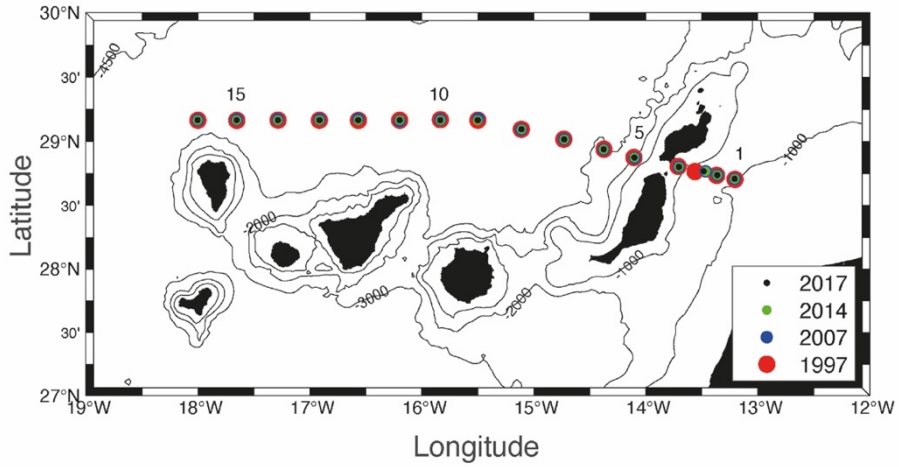

Figure 2. Hydrographic stations carried out during CANIGO (1997) and RaProCan (2007, 2014 and 2017)

The RaProCan and CANIGO spatial separation of each deep-water stations (located west of Lanzarote) was 35 km while in the shallower stations - east of Lanzarote - it got reduced to 15 km. For the RaProCan and CANIGO cruises, as stations are in the same position, temperature and salinity were only linearly interpolated onto a pressure grid with 10 dbar difference to have monotonically increasing density profiles.

The methodology applied to evaluate changes in temperature and salinity along the water column consists of two parts. First, differences are presented in vertical sections together with their zonal average to quantify the changes along each isoneutral layer. In the second part, the decomposition of this changes is done following the model proposed by (Bindoff & Mcdougall, 1994) where the variations in both pressure and density surfaces are related through the following equation:

$$\left.\frac{d\psi}{dt}\right|_z = \left.\frac{d\psi}{dt}\right|_{\gamma_n} - \left.\frac{dp}{dt}\right|_{\gamma_n} \frac{\partial\psi}{\partial p}$$

which represents the observed changes of the scalar quantity ψ along isobaric surfaces $\left(\left.\frac{d\psi}{dt}\right|_z\right)$ as the sum of two independent contributors, changes along neutral surfaces $\left(\left.\frac{d\psi}{dt}\right|_{\gamma_n}\right)$ and changes due to vertical displacement of the density surfaces $\left(\left.\frac{dp}{dt}\right|_{\gamma_n} \frac{\partial\psi}{\partial p}\right)$. This allows the comparison between the sum of the two decomposed components, which represents the warming and freshening (variation of the water mass) and the heaving of the isobaric changes.

3. Water Masses

Different water masses coexist in the Atlantic Ocean, cool and freshwater masses from polar regions, and warm and salty water masses created at low latitudes. However, not all water masses reach 24.5ºN and, to identify which ones are present at this latitude, a θ-S diagrams are used (Figure 3). Neutral densities defined by Hernández-Guerra et al., (2014) and Casanova-Masjoan et al., (2020) divide the water column into the different water masses. At the eastern boundary practically the same water masses as in 24.5ºN can be identified. Due to the anticyclonic behavior of the NASG (Hernández-Guerra et al., 2014), the isoneutrals present an inclination toward the west, making the depth of the water body vary from east to west, so in this section, the depth values will be used only as a reference.

Surface Waters (SW) are found from the surface down to the first 100 dbar, above the seasonal thermocline (γ^n<26.44 kg m^{-3};Casanova-Masjoan et al., 2020). These waters show scattering values, due to the seasonal evaporation, presence of fresh water, and the nearby coastal upwelling (Vélez-Belchí et al., 2017). Seasonal variability is seen in both cases (Table 1). For 24.5ºN (Figure 3a) summer (1981) values reach the highest temperatures and are more scattered than those ones of winter (1998 and 2015). For the

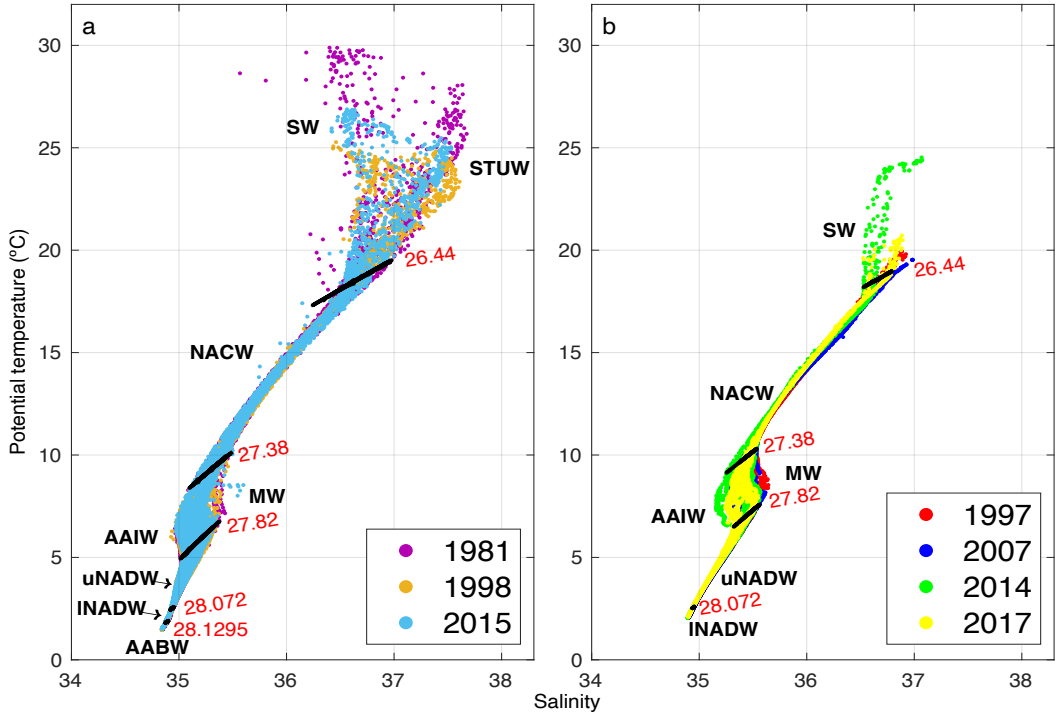

Figure 3. Θ-S diagrams for a) 24.5ºN cruises and b) CANIGO and RaProCan cruises. Black solid lines represent the g^n values (26.44, 26.85, 27.38, 27.82, 28.072 and 28.1295 kg m^{-3}) that define the different water masses in the region.

Canary Islands dataset (Figure 3b) temperature values show a clear temperature transition (from warmer to cooler) from early fall (2014) to mid-spring (2017) and to winter (1997 and 2007). A maximum of salinity between 23ºC and 26ºC (Figure 3a), corresponding to

the Subtropical Underwater (STUW) is also seen (Fu et al., 2017). This water mass originates in the subtropical Atlantic due to a region of high evaporation between 25ºW and 55ºW.

Below the SW, there is the thermocline, extending until 9ºC. The North Atlantic Central Water (NACW) is the main water mass of the thermocline (Pastor, M. et al., 2015; Benítez Barrios et al., 2008) This water mass is formed by winter subduction (Liu & Tanhua, 2021) and it is characterized by its linear potential temperature-salinity relationship (Harvey & Arhan, 1988). NACW extends from 100 dbar to 700 dbar and it's usually characterized with values of neutral density between 26.85 kg m^{-3} and 27.38 kg m^{-3}, it is the most abundant water mass of the NASG (Casanova-Masjoan et al., 2020).

Between 700 and 1400 dbar (27.38 kg $m^{-3} > \gamma^n <$ 27.82 kg m^{-3}) intermediate waters (IW) are found. Antarctic Intermediate Water (AAIW) and Mediterranean Water (MW) are the main water masses at this depth (e.g. Fraile-Nuez et al., 2010; Pérez-Hernández et al., 2013). These water masses are identified by their values of salinity and temperature, being AAIW cooler with a minimum in salinity, and MW warmer with a salinity maximum (e.g. Hernández-Guerra et al., 2017).

North Atlantic Deep Water (NADW) is the predominant water mas of the deep layers (27.82 kg $m^{-3} > \gamma^n <$ 28.1295 kg m^{-3}). NADW is found basin-wide and shows little variability (Figure 3). In the North Atlantic Ocean, NADW can be separated by upper and lower NADW that differentiate from each other by their neutral density and temperature values. uNADW is warmer (around 3.3ºC) than lNADW which has temperatures around 2.5ºC (Hernández-Guerra et al., 2014; Liu & Tanhua, 2021).

Below 4500 dbar ($\gamma^n >$28.1295 kg m^{-3}), the bottom layer is located. In this latitude, only the AABW (Antarctic Bottom Water) signal is seen. This water mass forms in Antarctica by subduction and flows northward along the western basin. Here, AABW is only seen at 24.5ºN and it is identified at the western flank of the Mid-Atlantic Ridge as in Bryden et al., (1996).

4. Results

4.1 Transoceanic θ/S isobaric changes

Figure 4 displays potential temperature and salinity differences and their zonal average for the transatlantic sections. The upper, central, and intermediate layers, the western and eastern stations show different trends, so has been deemed necessary to study each side of the basin individually making the division at 45ºW (Table 2). Deep and Bottom waters show basin-wide similar trends, so they will be considered together in Table 2.

Table 2. Zonally averaged temperature and salinity differences for the 24.5ºN cruises separated per water mass and basin (W and E). Differences are expressed in units of ºC decade^{-1} and decade^{-1} for potential temperature (light grey) and salinity (dark grey), respectively.

	SW				NACW				AAIW+MW				NADW+AABW			
	Pot. Temp		Sal		Pot. Temp		Sal		Pot. Temp		Sal		Pot. Temp		Sal	
	W	E	W	E	W	E	W	E	W	E	W	E	W	E	W	E
98-81	-0.38		0.061		0.12		0.023		0.13		0.008		0.01		0.000	
	-0.53	-0.22	0.068	0.053	0.06	0.18	0.016	0.030	0.11	0.16	0.007	0.020	0.00	0.02	-0.002	0.002
15-98	0.22		-0.053		0.02		0.001		-0.02		-0.003		-0.01		-0.002	
	0.58	-0.15	-0.014	-0.092	0.02	0.02	0.000	0.001	-0.05	0.01	-0.005	0.000	-0.01	0.00	-0.002	-0.002
15-81	-0.06		0.005		0.07		0.011		0.06		0.006		0.00		-0.001	
	0.04	-0.17	0.026	-0.016	0.04	0.09	0.007	0.014	0.03	0.08	0.001	0.010	0.00	0.01	-0.002	0.000

SW (γ^n <26.44 kg m^{-3}) show a generalized cooling throughout the layer of -0.38ºC decade^{-1}, accompanied by an increase in salinity of 0.061 decade^{-1} in the 1981-1998 period (Table 2, and Figure 4a, d, e, and h). This cooling occurs in the first 100 dbar, and it is better sensed at the eastern basin due to the eastward shoaling of the isopycnal (Figure 4a). A strong warming is observed below 100 dbar (Figure 4a to d). For the following period (1998-2015), cooling is observed only east of 40ºW (-0.15ºC decade^{-1}, Table 2 and Figure 4i, and k). This is not observed in the zonally averaged temperature differences due to the warming that expands all over the western zone of the basin (which is of 0.58ºC decade^{-1}) (Table 2, and Figure 4i, j and l). In salinity, a freshening of -0.053 decade^{-1} is observed, being stronger on the eastern side of the basin (Table 2, and Figure 4 m to p). The global trend (2015-1981) shows for SW, a cooling of -0.06ºC decade^{-1}, influenced by the upper cooling that occurred from 1981 to 1998 (Table 2, Figure 4q *versus* Figure 4a). Looking at the trends on each side of the basin under the cool upper layer, the pattern also resembles that of the 1998-2015, with warming at the western basin and cooling at the eastern basin (Figure 4q *versus* Figure 4i). The total SW zonally averaged salinity differences show a mild increase in salinity. However, this increase is only observed in the western basin (0.026 decade^{-1}) as in the east a decrease in salinity of -0.016 decade^{-1} occurs (Figure 4 u to x, and Table 2).

NACW (26.85 kg m^{-3} > γ^n < 27.38 kg m^{-3}), presents a warming of 0.12°C decade^{-1} from 1981 to 1998, accompanied by an increase in salinity of 0.023 decade^{-1} (Table 2, Figure 1a, d, and h). A great warming and salinity increase is observed in the westernmost side of the basin (70ºW to 75ºW) even reaching intermediate levels. This warming is followed by a cooling and freshening between 50ºW to 70ºW (Figure 4a, b, e, and f). At the eastern basin, warming and salinification occupies practically the entire layer and drives the overall zonal average (Figure 4a to h, and Table 2). These are particularly strong at the easternmost stations (Figure 4a and e) For the 1998-2015 time-span, a warming and an increase in salinity is also observed, but of an order lower than in the previous period (Figure 4i to p). Both the western and eastern sides of the basin show the same warming trend of 0.02ºC decade^{-1}, while in salinity, the increase is only visible at the eastern stations (0.001 decade^{-1}, Table 2). Finally, the 34-year difference shows a temperature

and salinity trend of 0.07ºC decade^{-1} and 0.011 decade^{-1} respectively, clearly driven by the eastern basin and the 1981-1998 period (Table 2).

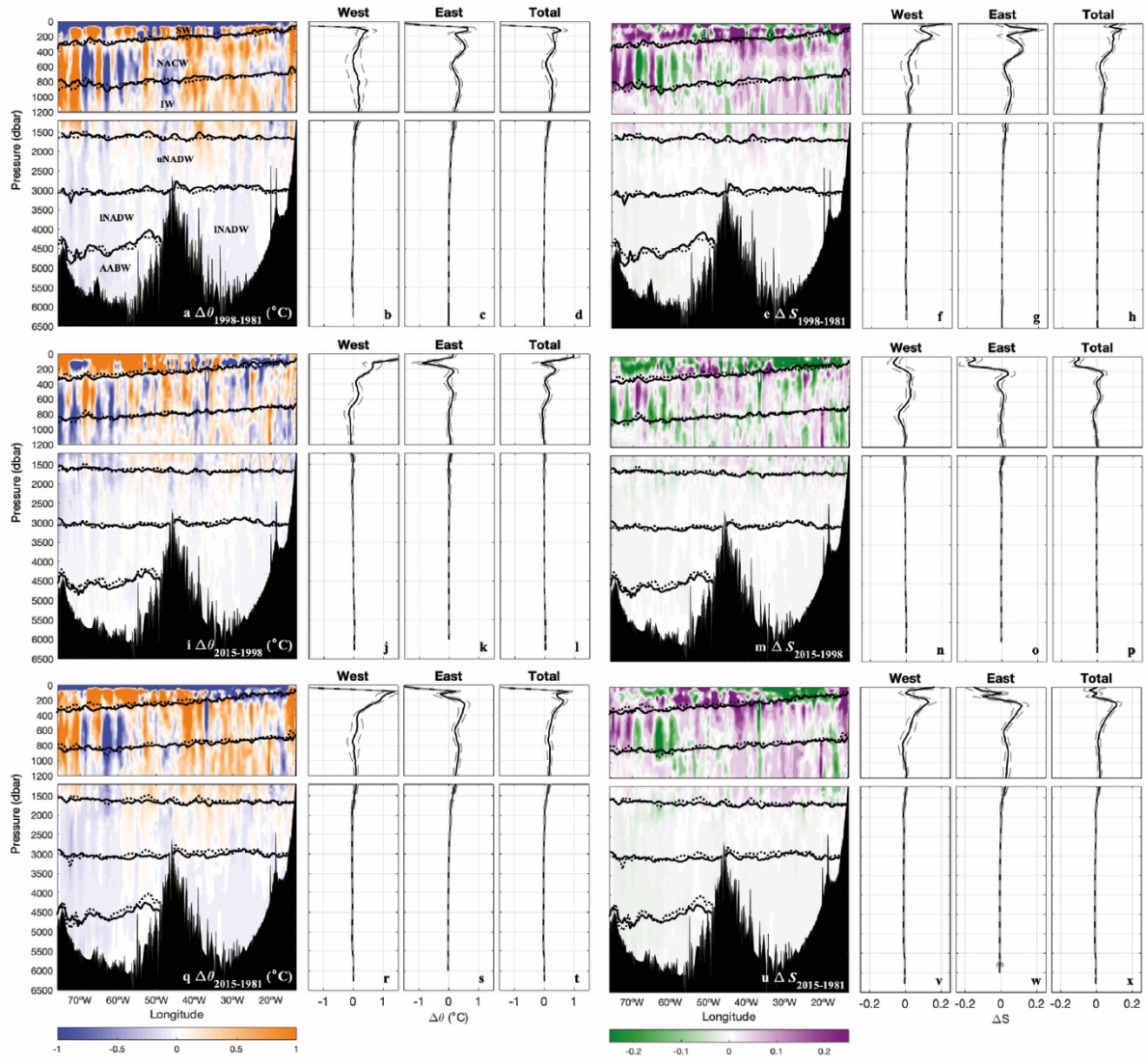

Figure 4. A05 Vertical sections of potential temperature (left column) and salinity (right column) together with their eastern, western and total zonally averaged profile for the (a to h) 1998-1981, (i to p)2015-1998, and (q to x)2015-1981 differences. Overayed in all figures, reprentative densities for each of the water masses marked in a, have been plotted in grey (black) for the initial (final) date of the difference.

At Intermediate Waters (27.38 kg m^{-3} > γ^n< 27.85 kg m^{-3}), increasing values of temperature and salinity are seen from 1981 to 1998 (Figure 4 a, to h). These occur at a rate of 0.13ºC decade^{-1} and 0.008 decade^{-1}, respectively, being a little higher at the eastern stations (Table 2). A change in trend is observed in the following period (1998 to 2015), where a mild decrease in both temperature (-0.02ºC decade^{-1}) and salinity (-0.003 decade^{-1}) is observed (Figure 4 i to p). As seen on Figure 4 and Table 2, these decreases are mainly occurring at the western stations. The 2015-1981 difference shows an increase in the two variables, being higher in the eastern basin in both cases (Table 1). The global

mean presents mild temperature and salinity increasing rates of 0.06ºC decade^{-1} and 0.006 decade^{-1}.

Both NACW and IW, show an extensive warming at the western basin (70ºW to 75ºW) in the 1981-1998 and 2015-1981 differences that disappears in the 2015-1998 period. As in the upper layers, at intermediate depths the 1998-1981 period leads the 2015-1981 trend.

Deep and Bottom Waters (> 3000 dbar) present very weak trends (Table 2 and Figure 4). An increase in temperature from 1981 to 1998 of 0.01ºC decade^{-1} is observed. This trend reverses on the following period (1998 to 2015) and comes with a mild decrease in salinity (-0.002 decade^{-1}). Nonetheless, the 34-year difference does not reflect significant changes in temperature, but a slight decrease in salinity (Table 2, Figure 4 t, and x). This freshening occurs in the western side of the basin (Figure 4u, v, and w). While in the east the temperature increases 0.01ºC decade^{-1} (Figure 4 q, r and s).

4.2 θ/S isobaric changes at the Eastern boundary of the NASG

Figure 5 presents a zoom of the above A05 sections differences at the Eastern boundary of the NASG. The highest changes, as in the transatlantic section, are seen in the 1998-1981 difference, imprinting a remarkable bipolar pattern in the overall difference (Figure 5 a, c, i and k). For both periods, from 0-2000 dbar warming expands from 13º to 16ºW (0.22ºC decade^{-1} in 1998-1981, and 0.13ºC decade^{-1} in 2015-1981), followed by a weaker cooling covering from 16º to 18ºW (-0.06ºC decade^{-1} in 1998-1981, and -0.05ºC decade^{-1} in 2015-1981). Salinity follows the same pattern (Figure 5 e and k), showing increases at the eastern side (0.047 decade^{-1} in the 1998-1981 difference, and 0.024 decade^{-1} in the 2015-1981), while freshening takes place at the western stations (-0.01 decade^{-1} in both periods).

The 2015-1998 difference is under a higher mesoscale activity than the other two periods, however it shows a clear warming in NACW at a rate of 0.08ºC decade^{-1} together with an increase in salinity of 0.010 decade^{-1} (Figure 5 e, to h). In addition, at intermediate level, a cooling of -0.11ºC decade^{-1} and a freshening of -0.003 decade^{-1} occurs.

As reported in the introduction, most of the variability at the eastern boundary is driven by the upper and intermediate layers. Thus, the total zonally averaged difference in deep waters show a weak warming in all differences of 0.01ºC decade^{-1}. Salinity in the 1998-1981 and 2015-1998 differences present opposing trends of 0.002 decade^{-1} and -0.04 decade^{-1}, respectively.

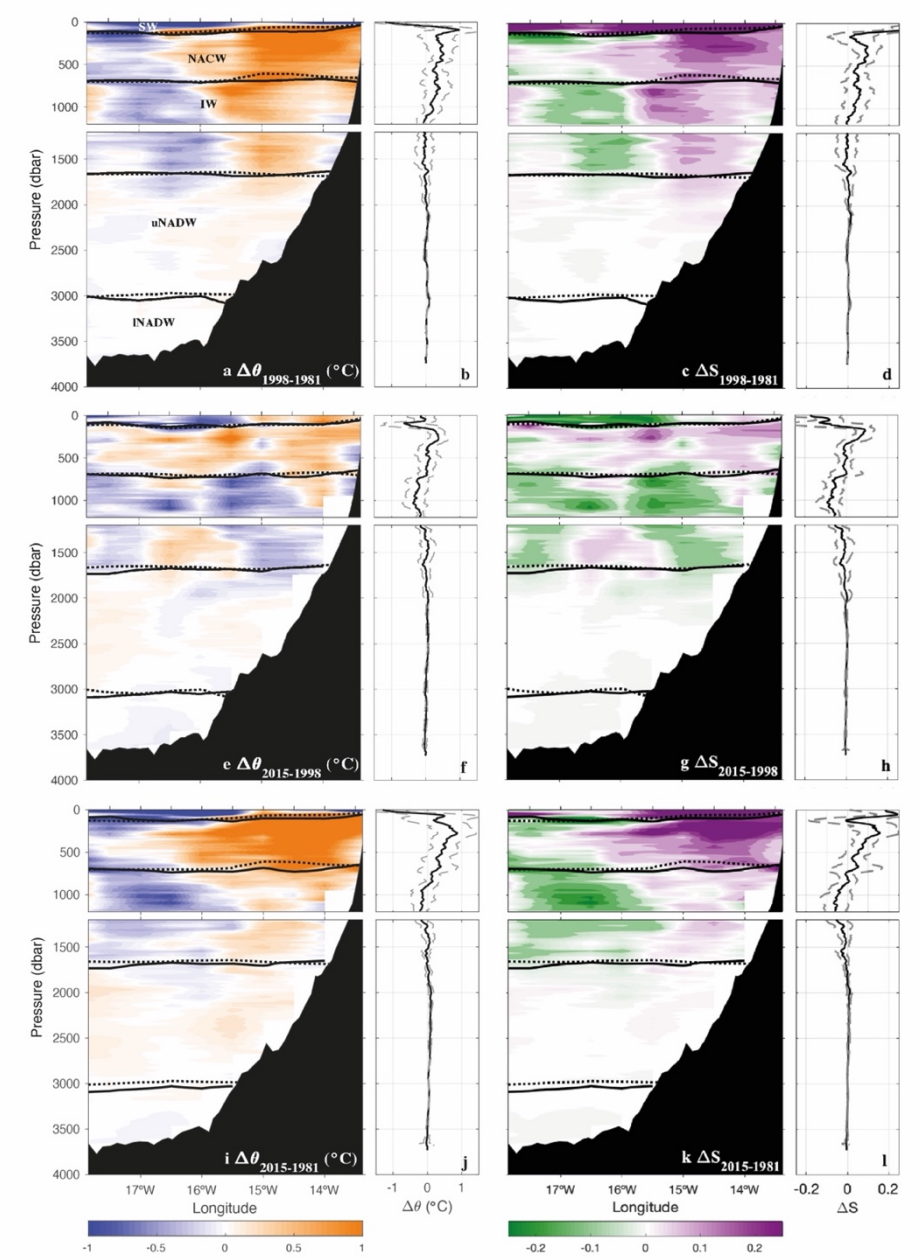

Figure 5. Eastern boundary A05 vertical sections of temperature (left column) and salinity (right column) differences for (a to d) 1998-1981, (e to h) 2015-1998, and (i to l) 2015-1981. Overayed in all figures, reprentative densities for each of the water masses marked in a, have been plotted in grey (black) for the initial (final) date of the difference.

The latest results are located south of the Canary archipelago, in an area of high mesoscale activity. Therefore, to further explore interannual changes at the eastern boundary of the NASG, the high-resolution CANIGO and RaProCan cruises, located north of the Canary Islands, will be used. In addition, results for these cruises will be divided into a Coastal Transition Zone (CTZ, stations 1 to 10) and an open ocean zone (OO, stations 11 to 16). The CTZ will be influenced by the nearby African upwelling and the Canary intermediate Poleward Undercurrent (CiPU; Vélez-Belchí et al., 2021).

While the east to west bipolar pattern described above reaches all the way from 2000 dbar to the surface in the A05, this is not the case north of the Canary Islands, where the surface layer behaves more homogenously (Figures 6 and 7). A clear cooling (-0.10ºC decade^{-1}) and freshening (-0.007 decade^{-1}) in the NACW OO stations is observed only in the 2007-1997 period (Figures 6a and b and 7a and b). However, this cooling does not affect the zonally averaged difference (Figure 6d and 7d). For the following periods, the overall mean shows warming and salinification (Figures 6 and 7, e to p). In Figures 6 and 7, it is noticeable that all the NACW zonally averaged temperature and salinity differences show increases except the 2007-1997 period. This is due to 2014, which was an anomalously warm and salty year (Figure 6m and 7m). Consequently, an averaged warming of 0.2°C decade^{-1} is observed for the 2017-2007 and 2014-1997 differences, and a maximum salinification of 0.015 decade^{-1} in 2014-1997.

Nevertheless, the bipolar pattern of the A05 is still observable in the 1997-2017 difference, but with less intensity and constraint only from 100 to 1500 dbar (Figure 6i and Figure 7i). One can think that this pattern could be showing seasonal variability, however, while the pattern appeared for the A05 winter minus summer differences, in this case, the pattern appears between a spring and a winter cruise, suggesting a persistent interannual trend. This is true for the warming as an average trend of 0.1ºC decade^{-1} is observed for both the 2015-1981 and 2017-1997 differences. However, the increase in salinity is an order of magnitude weaker (0.05 decade^{-1}) north of the islands in the overall 2017-1997 period.

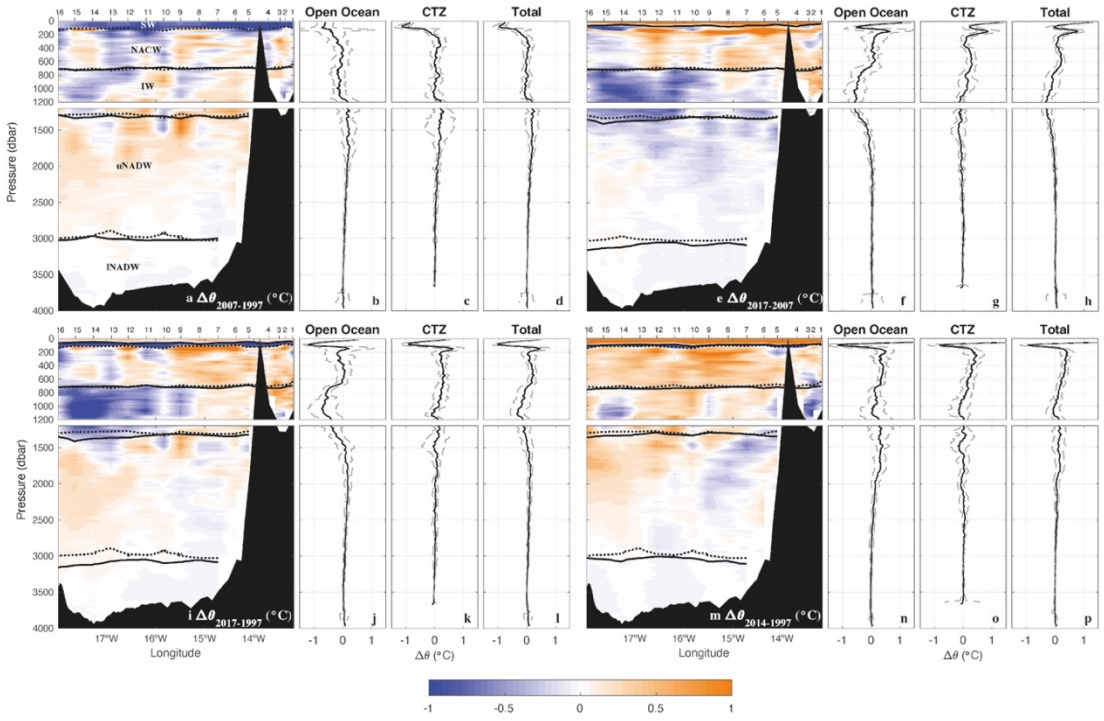

Figure 6. Vertical profiles for the CANIGO and RaProCan cruises and their zonally average profile (Open Ocean, Coastal Tranzition Zone and Total) of potential temperature for (a to d) 2007-1997, (e to h) 2017-2007, (i to l) 2017-1997, and (m to p) 2014-1997.

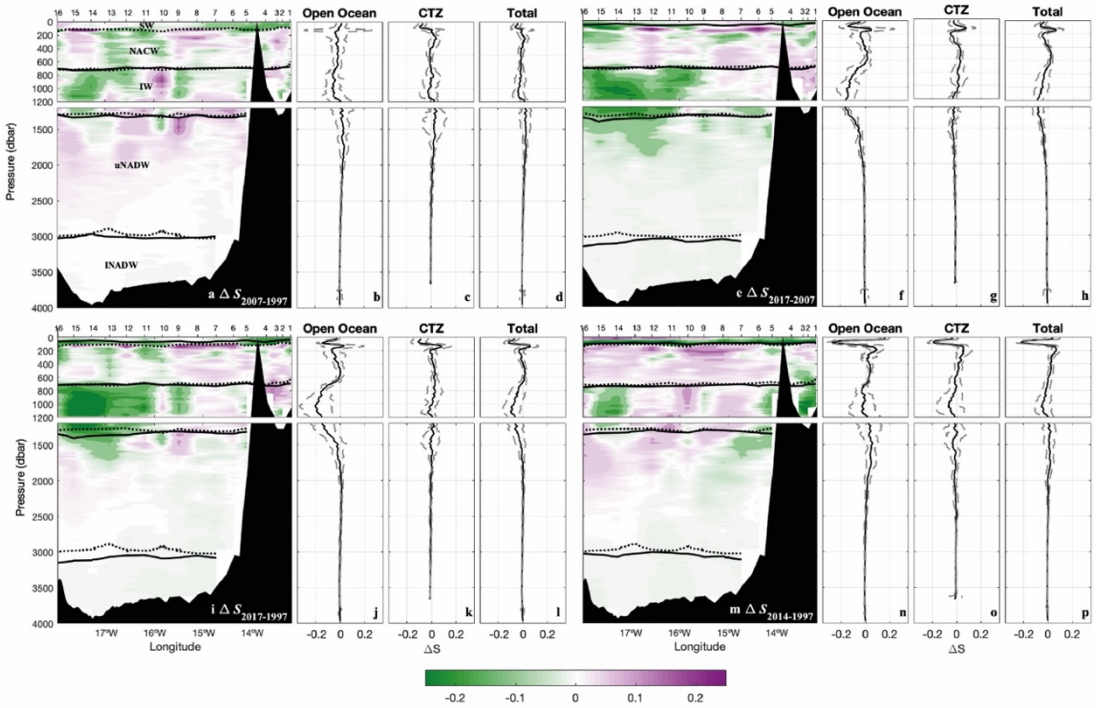

Figure 7. Vertical profiles for the CANIGO and RaProCan cruises and their zonally average profile (Open Ocean, Coastal Tranzition Zone and Total) of salinity for (a to d) 2007-1997, (e to h) 2017-2007, (i to l) 2017-1997, and (m to p) 2014-1997.

Intermediate waters present greater variability, so the confidence interval widens, and the results became less statistically significant. In the OO, both north and south of the Canary Islands a cooling and freshening is observed in all differences, suggesting a weaking of the MW salinity signal (Figures 5, 6, and 7, this is also observable in Figure 2). This decreasing trend is stronger north of the Canary Islands (-0.29ºC decade^{-1} and -0.087 decade^{-1} for both temperature and salinity, respectively) than in the A05 (-0.07ºC decade^{-1} and -0.002 decade^{-1} for both temperature and salinity, respectively). The northern section is closer to the Mediterranean Sea and less perturbed by downstream island-effects. In contrast, the 2014 cruise took place in fall, when the CiPU is active, hence when a higher contribution of AAIW takes place (Knoll et al., 2002; Vélez-Belchí et al., 2021). This generates at the bottom of the Lanzarote Passage a cool and fresh patch in Figures 6m and o, and 7m and o).

A warming and salinization in the open ocean stations up to 2500 dbar is seen in Deep waters, except for the 2017-2007 difference, where cooling is seen (Figure 6 and 7 a, e, i, and m). For the first period (1997 to 2007) all NADW warmed at a same rate (0.09ºC decade^{-1}) accompanied by an increase in salinity of 0.013 decade^{-1}. The following period, however, shows a change in trend of -0.04ºC decade^{-1} and -0.017 decade^{-1} respectively. The total difference (2017-1997), shows a warming, being higher in the OO stations area (0.05ºC decade^{-1}) than in the CTZ (0.01ºC decade^{-1}). As for salinity, a decrease occurs from 1997 to 2017 in the whole layer of 0.002 decade^{-1}. When comparing with 2014 (Figures 6 and 7 m to p), a warming in the OO stations (0.04ºC decade^{-1}) accompanied

by an increase in salinity (0.005 decade^{-1}) is observed, while in the CTZ stations only a freshening of -0.008 decade^{-1} is seen.

4.3 Bindoff and McDougall (1994) decomposition at the A05 transoceanic section

Results from applying the Bindoff and McDougall (1994) show for all differences that the sum of the components (green line) compares well with the isobaric change (black line). This indicates that the decomposition of the isobaric change has been done successfully. At surface, the high variability and dispersion of the values lead to non-significant results, so the Bindoff and McDougall (1994) results are enabled at 150 dbar.

For NACW (roughly from 150 to 900 dbar), the warming an increasing salinity seen in the first period (1998-1981) generates a temperature-driven deepening of the isoneutrals where the largest contributor is the eastern basin (Figure 8 a to f). In the following period (1998 to 2015) both basins contribute to the total profile. The total profile is mainly driven by temperature changes at the western boundary as it presents a similar shape, however the eastern boundary contributes to the roughly 300 dbar shoaling and to the 600 dbar deepening (Figure 8 g to l). The global 2015-1981 difference shows that the overall warming comes with a temperature-driven deepening of the isoneutrals (Figure 8 m to o). Tough the eastern boundary is the main contributor to this deepening; the western boundary leads between 150 dbar to roughly 300 dbar.

At intermediate levels (800-1500 dbar) an increase in temperature and salinity is observed in the global decomposition accompanied with a deepening of the isopycnals (Figure 8 m to r). These changes are led by the first period where temperature at the western basin drives a deepening of the isoneutrals (Figure 8 a to f). The second period shows no significant changes in the decomposition.

NADW and AABW present not significant changes except from 1981 to 2015, where two deepening of the isoneutrals is observed. The first one has its source on an eastern boundary temperature driven change that expans from 1500 dbar to roughly 3000 dbar (figure 8 m and o). While the second is due to both temperature and salinity from 4000 to 5000 dbar, which occurs mainly in the western half of the Nort Atlantic basin (Figure 8 m, o, p and r).

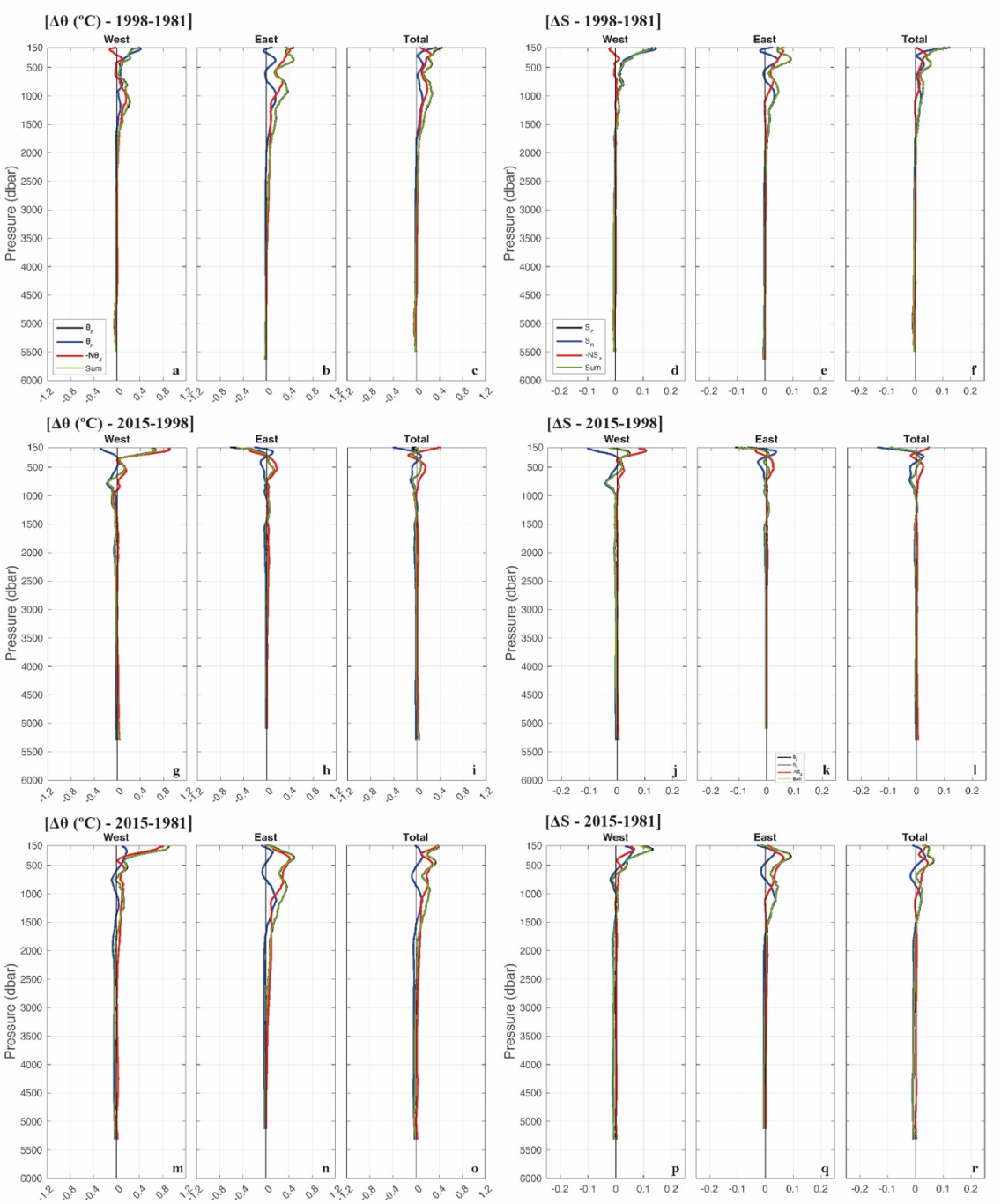

Figure 8. A05 results from the Bindoff and McDougall (1994) decomposition. Isobaric changes ($\theta'|_z$ and $S'|_z$ black) are decomposed into changes along neutral surfaces ($\theta'|_n$ and $S'|_n$ blue) and changes due to the vertical displacement of the isoneutrals ($-N\theta_z$ and $-NS_z$ red) for temperature (left column) and salinity (right column). The decomposition has been done for the eastern and western basins, and total in (a to f) 1998-1981, (g to m) 2015-1998, and (n to s) 2015-1981 differences.

4.4 Bindoff and McDougall (1994) decomposition at the Eastern boundary of the NASG

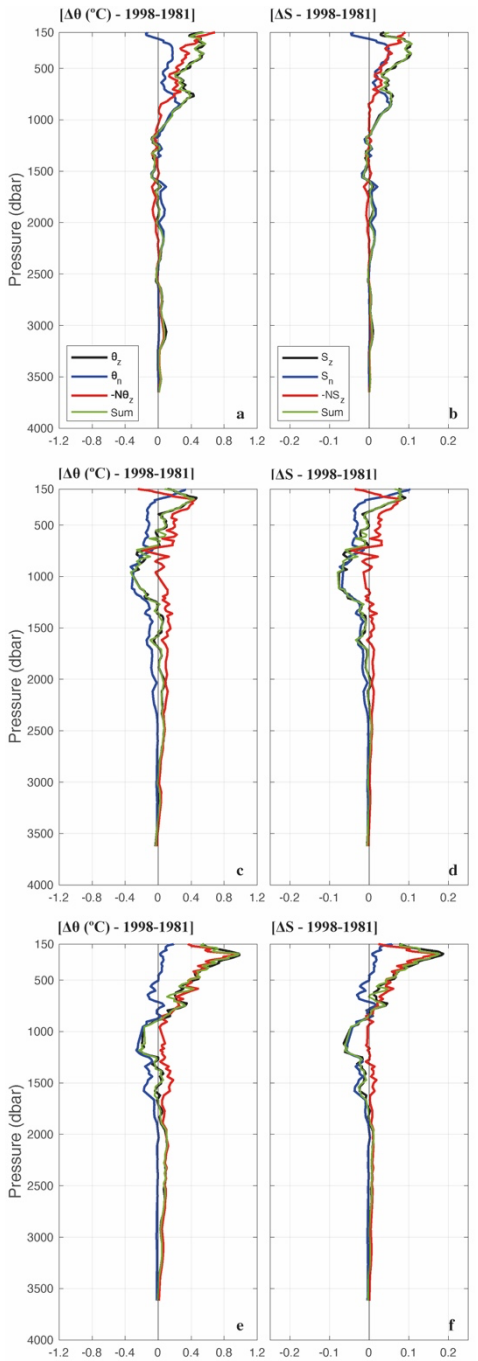

Figure 9. Eastern boundary A05 isobaric changes ($\theta'/_z$ and $S'/_z$ black) decomposed into changes along neutral surfaces ($\theta'/_n$ and $S'/_n$ blue) and changes due to the vertical displacement of the isoneutrals ($-N\theta_z$ and $-NS_z$ red) for temperature (left column) and salinity (right column) differences for (a,b) 1998-1981, (c,d) 2015-1998, and (e,f) 2015-1981.

For the stations south of the Canary Islands (A05 sections) the warming and the increase in salinity seen from 1981 to 1998 generates a temperature-driven deepening of the isoneutrals up to 1000 dbar (Figure 9 a and b). For the next period (2015-1998) a temperature-driven deepening of the isoneutrals is also seen but reaches up to 2500 dbar (Figure 9 c and d). In this period, the cooling and salinity decrease in intermediate waters (700-1400 dbar) are due to changes along the isoneutrals (Figure 9 c and d). The 34-year difference (2015-1981 period) reflects the deepening of the isoneutrals seen in both periods, and the cooling and freshening of intermediate waters seen in the 2015-1981 period (Figure 9 e and f).

For the northern sections, a temperature-driven deepening of the isoneutrals is seen for central waters in all the differences except the first period (2007-1997), where shallowing generates all the changes (Figure 10 and 11). This is also seen in Figures 6a and 7a, where the 26.44 kg m^{-3} (SW) isoneutral disappears in 2007. For intermediate waters, most of the changes are due to changes in the water mass properties, due to the alternating presence of MW and AAIW. The warming seen for NADW in all periods except for the 2017-2007, is due to a temperature-driven deepening of the isoneutrals. In the 2017-1997 period both contributors generate the changes. The only difference that shows a generalized warming is 2014-1997. This warming generates a temperature-driven deepening of the isoneutrals. Deep water warming in 2014, could be the main contributor to the warming of these waters in the period 2017-1997 (mostly at OO stations), as prior to 2014 this warming is minor (Figure 10 a, d, g, and j).

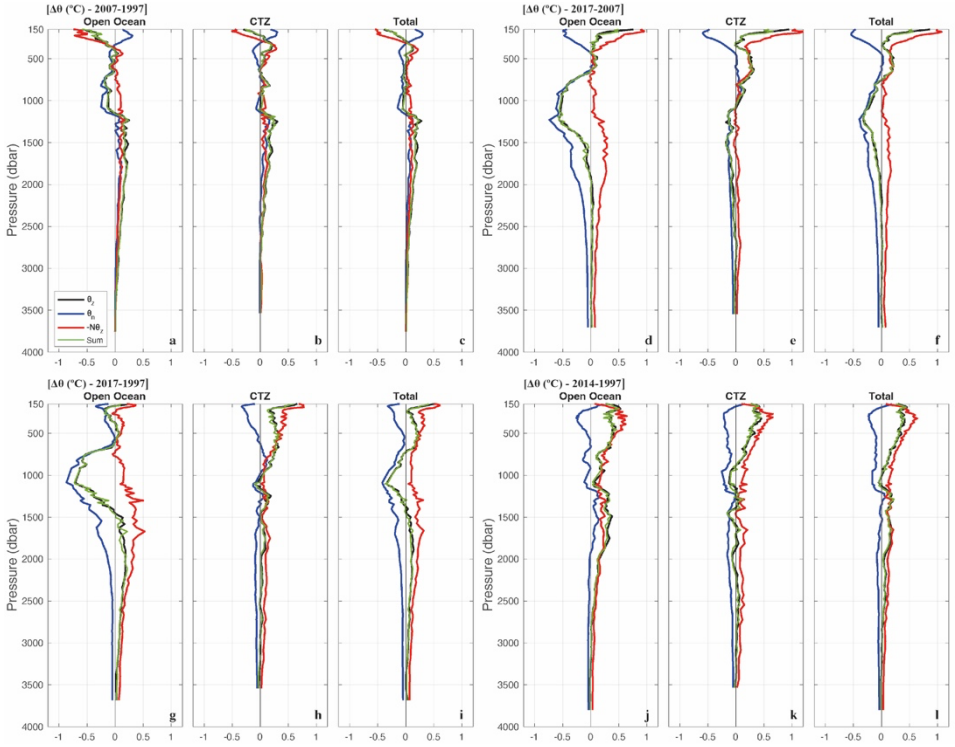

Figure10.Isobaric changes ($\theta'|_z$ and $S'|_z$ black) decomposed into changes along neutral surfaces ($\theta'|_n$ and $S'|_n$ blue) and changes due to the vertical displacement of the isoneutrals ($-N\theta_z$ and $-NS_z$ red) for the CANIGO and RaProCan cruises and their Open Ocean, CTZ and Total profile of potential temperature for (a to d) 2007-1997, (e to h) 2017-2007, (i to l) 2017-1997, and (m to p) 2014-1997.

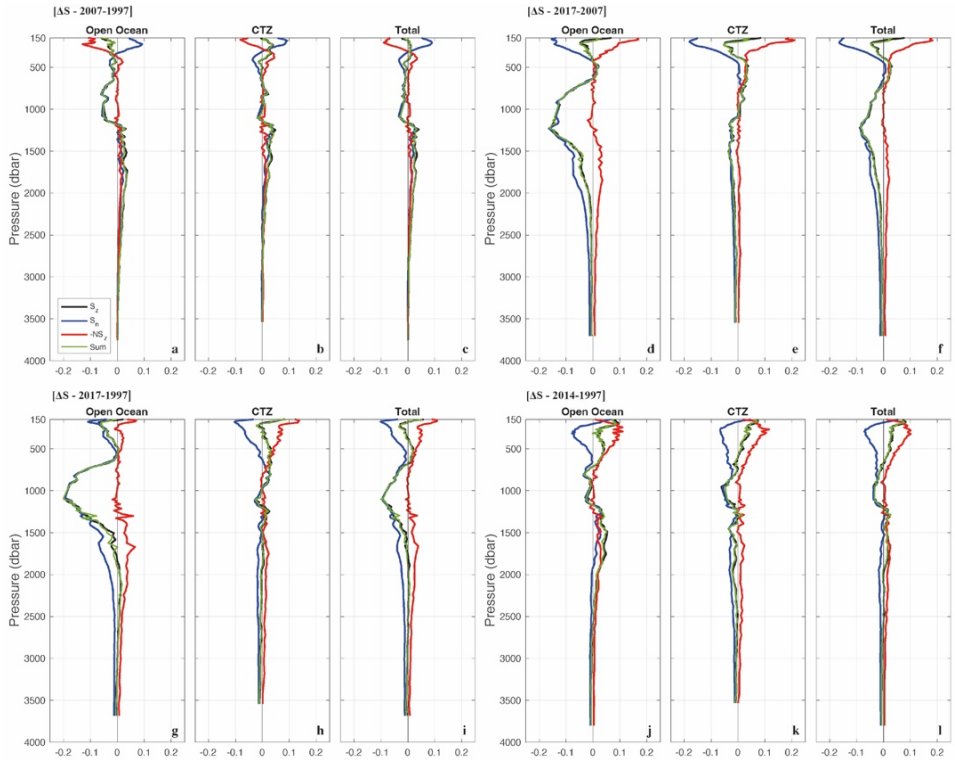

Figure 11. Isobaric changes ($\theta'|_z$ and $S'|_z$ black) decomposed into changes along neutral surfaces ($\theta'|_n$ and $S'|_n$ blue) and changes due to the vertical displacement of the isoneutrals ($-N\theta_z$ and $-NS_z$ red) for the CANIGO and RaProCan cruises and their Open Ocean, CTZ and Total profile of salinity for (a to d) 2007-1997, (e to h) 2017-2007, (i to l) 2017-1997, and (m to p) 2014-1997.

5. Discussion

Over 34 years, the interannual and seasonal variability of the water masses existing on the NASG, and its eastern boundary are studied here from hydrographic data. Changes in water masses are explored by applying the model proposed by Bindoff and McDougall (1994), where changes are attributed to changes along neutral surfaces and changes due to vertical displacement of isoneutrals.

Table 3. Comparison between our results (highlighted in bold) and previous studies for the A05 cruises where each super index corresponds to: (1) Vélez-Belchí et al., 2010, (2) Cunninham & Alderson (2008), (3) Vargas-Yáñez et al., 2004, and (4) Parrilla et al., 1994

Period	Depth	Temperature (ºC decade^{-1})		Salinity (decade^{-1})		Isobaric Change
		West	East	West	East	
1981-1998	**150-700**	**0.12**		**0.023**		**deepening**
1998-2015	**150-700**	**0.02**		**0.001**		**deepening**
2015-1981	**150-700**	**0.07**		**0.011**		**(deepening and property changes)**
1957-1981[1]	300-800	0.14		-		deepening
1957-1998[1]	300-800	0.24		-		deepening
1998-2004[1]	300-800	-0.15		-0.130		shallowing
1957-2004[2]	300-800	0.11	0.03	0.020	0.003	deepening
1992-2002[3]	100-1000	0.27		0.024		deepening
1957-1992[4]	1100	0.32 (max.)		-		deepening
1981-1998	**700-1400**	**0.13**		**0.008**		**deepening**
1998-2015	**700-1400**	**-0.02**		**-0.003**		**-**
2015-1981	**700-1400**	**0.06**		**0.006**		**-**
1957-1981[1]	800-1800	0.14		-		deepening
1957-1998[1]	800-1800	0.27		-		deepening
1998-2004[1]	800-1800	-0.13		-0.130		shallowing
1957-2004[2]	900-1750	0.07	0.01	0.004	-0.002	heave/property changes
		-0.02	-0.01	-0.003	-0.002	shallowing
1981-1998	**>1400**	**0.01**		**-**		**deepening**
1998-2015	**>1400**	**-0.01**		**-0.002**		**deepening**
2015-1981	**>1400**	**-**		**-0.001**		**deepening**
1957-1992[4]	3000	-0.1 (max.)		-		-
1957-2004[2]	>4000	-0.02	-	-0.003	-	-

For NACW (150-900 dbar), between 1957-1981 a warming of 0.14ºC decade^{-1} was found in Vélez-Belchí et al., (2010). A trend that following our results, persisted until 1998, and that was in both cases, due to a temperature-driven deepening of the layer. At least in our 1981-1998 difference, these changes were mainly driven by the eastern boundary. This is consistent with the findings of Vargas-Yáñez et al., (2004) where they attributed the warming from 1992 to 2002 between 350 dbar and 1000 dbar to a deepening of the

isoneutrals. Furthermore, results from Cunningham & Alderson (2007) suggest that this increasing trend could be consistent until 2004. In contrast, Vélez-Belchí et al., (2010) presented a trend that doubled our estimations between 1957 and 1998 and that lies closer to the trend of Vargas-Yáñez et al., (2004) for the eastern side of the basin. However, this 0.24ºC decade $^{-1}$ from Vélez-Belchí et al., (2010) gets balanced by a cooling between 1998 to 2004, reinforcing this 0.1ºC decade $^{-1}$ trend from 1957 to 2004. Later in our study, between 1998 and 2015 we find a very weak warming, followed again by a 0.1ºC decade $^{-1}$ trend from 1981 to 2015. In addition, all of these publications agree that the NACW layer is deepening from 1957 to 2015, with the exception of the Vélez-Belchí et al., (2010) 1998 to 2004 period.

Likewise, the salinity at the NACW level shows an increase of 0.023 decade $^{-1}$ for the 1981-1998 period in our study. This trend is support by the ones estimated in Cunningham & Alderson (2007) for the 1957-2004 period and in Vargas-Yáñez et al., (2004) for the eastern side of the basin. Nevertheless, this increase in salinity has slowdown in the latest years to 0.011 decade $^{-1}$.

A consistent warming was observed in Figure 4 at the easternmost side of the basin. This was confirmed with the dataset from RaProCan and CANIGO where a trend slightly higher that of the full basin (of 0.2ºC decade^{-1}) is observed between 1997 and 2017. A trend that agrees with that of Vélez-Belchí et al. (2015) estimations for the eastern basin. The cooling and freshening seen by Benítez-Barrios et al., (2008) from 1997 to 2006 (350-600 dbar; Table 4) is also observed from 1997 to 2007. However, our results show that the waters have cooled and freshened at a rate of -0.79ºC decade^{-1} and -0.034 decade^{-}

Table 4. Comparison between our results (highlighted in bold) and previous studies for the eastern boundary sections where each super index corresponds to: (1) Benítez-Barrios et al., 2008, and (2) Vélez-Belchí et al., 2015.

Period	Depth	Temperature (ºC decade-1)		Salinity (decade-1)		Isobaric Change
		West	East	West	East	
1997-2006[1]	100-350	-0.26		-0.070		-
1997-2014[2]	200-600	0.20		0.030		-
1997-2007	**150-700**	**-0.79**		**-0.034**		shallowing
2007-2017	**150-700**	**0.20**		**-**		deepening
1997-2014	**150-700**	**0.20**		**-**		deepening
1997-2017	**150-700**	**0.20**		**0.015**		deepening
1997-2014[2]	1500-2300	0.32		0.052		deepening
1997-2007	**>1400**	**0.09**		**0.013**		-
2007-2017	**>1400**	**-0.04**		**-0.027**		deepening
1997-2014	**>1400**	**0.04**	**-**	**0.005**	**-0.008**	deepening
1997-2017	**>1400**	**0.05**	**0.01**	**-0.002**		deepening and property changes
1997-2006[1]	1600	0.29 (max.)		0.047 (max.)		-
1997-2014[2]	2600-3600	-0.01		-0.002		-

^{1} unlike that found by Benitez-barrios et al., 2008 (-0.26ºC decade^{-1} and -0.070 decade^{-1}). This decrease is produced by a shallowing of the isoneutrals in 2007. In the periods reported here, both mechanisms contribute to the changes.

It is also important to note that the warming and cooling seen at the western boundary extending from surface to intermediate layer at 24ºN could be the signal of the Antilles current. This current is the western boundary of the NASG. The observed warming occurs during the boreal winter (1998 and 2015), time of the year when the AMOC has a transport peak. While in 1981 (boreal August) the AMOC reaches a minimum (Fu et al., 2017). It is also noteworthy to mention that the years 1998 and 2015 are years known as strong El Niño years (Yu et al., 2020). So the similarities between the 1981-1998 and 1981-2015 profiles along with the decrease in surface temperature could be due to this phenomenon, although it needs further investigation.

As in the thermocline layer, at intermediate levels (800-1500dbar) a consistent warming of 0.1ºC decade^{-1} is observed from 1957 to 2004 when considering Vélez-Belchí et al. (2010) (1957-1981 and the sum of the 1957-1998 and 1998-2004 trends), our study (1981-1998), and Cunningham & Alderson (2007) (1957-2004). Though while a deepening of the layer is observed in our study and Vélez-Belchí et al. (2010), in Cunningham & Alderson, (2007) they attribute the changes to heave and property changes along the layer. For salinity there is an increase observed in our 1981-1998 and 2015-1981 periods and to a lower extend in the Cunninham and Alderson (2007) 1957-2004 difference, but the overall trend is hard to infer.

North of the Canary Islands, seasonality is seen in Intermediate Waters. In this layer two water masses alternate, in winter (1997 and 2007) MW is found in the open ocean stations by the presence of Meddies, and in fall (2014) there is an AAIW. This has been widely reported on the literature (Casanova-Masjoan et al., 2020; Fraile-Nuez et al., 2010; Hernández-Guerra et al., 2017).

Of all the vertical difference profiles studied, the 2014-1997 difference is the only one that shows warming practically throughout the whole water column. This temperature increase could be due to a Marine Heat Wave. Hobday et al., (2016) defined Marine Heat Wave as anomalously warm events, exceeding the seasonal threshold for at least 5 consecutive days. This phenomenon was observed in the Canary Islands area in 2014 for almost 50 days (Acuña & Izquierdo, 2021).

At the deeper layers Cunninham and Alderson (2007) found a cooling and freshening at the western basin. Our temperature changes for 1998-2015 are consistent with them but not the for the previous period. Similarly occurs with salinity. The NADW warming seen by Benítez-Barrios et al., (2008) and Vélez-Belchí et al., (2015) is also observed in our study at the eastern basin. In our case it reaches the bottom at a rate of 0.03ºC decade^{-1},

however a decrease in salinity of -0.002 decade^{-1} is observed. The warming in NADW is driven by a deepening in the isoneutrals while the freshening is due to a changes in the water mass properties, consistent with a freshening of the sub-polar North Atlantic reported by Curry & Mauritzen (2005) and also mentioned in Vélez-Belchí et al., (2015).

6. Conclusions

This study represents the largest study on interannual water masses characteristics at the eastern boundary of the North Atlantic Subtropical Gyre. The main conclusions of the study are:

- NACW (150-900 dbar) has warmed consistently between 1957 and 2015 at a rate of a warming of 0.1ºC decade^{-1}. This warming comes with a temperature-driven deepening of the water mass and is strongly influenced by the changes at the eastern basin. At the Eastern boundary the NACW trend slightly higher that of the full basin (of 0.2ºC decade^{-1}) is between 1997 and 2017. The salinity at the NACW level shows an increase of 0.02 decade $^{-1}$ from 1957 to 2004 but this increase in salinity has slowdown in the latest years to 0.011 decade $^{-1}$.
- At intermediate levels (800-1500dbar) a consistent warming of 0.1ºC decade^{-1} is observed from 1957 to 2004 but for salinity the overall trend is hard to infer. North of the Canary Islands, the high seasonality impedes the estimation of a clear trend. However, a decreasing of the MW properties (-0.3ºC decade^{-1} and -0.09 decade^{-1}) is observed between 1997 and 2017.
- The variability of the upper ocean (0 – 1500 dbar) in the 24.5ºN section, can be attributed to large-scale processes like El Niño. While in the eastern boundary the seasonality plays a major role in the variability of these Water Masses.
- The Antilles Current can be imprinting an intermittent signal at the western side of the basin (50-75ºW) at certain years.
- In the dataset located north of the Canary Islands 2014 seems to be a particularly warm year (possibly an MHW) and presents AAIW due to the CiPU.
- At the deeper layers we found a weak cooling and freshening.

7. Bibliography

Acuña, L. C., Izquierdo, A. & Cianca A. (2021). *Caracterización de las Marine Heat Waves (MHW) u olas de calor marinas en la cuenca canaria*. 47. Trabajo de Fin de Grado. Universidad de Cádiz. https://rodin.uca.es/handle/10498/25569

Benítez-Barrios, V. M., Hernández-Guerra, A., Vélez-Belchí, P., Machín, F., & Fraile-Nuez, E. (2008). Recent changes in subsurface temperature and salinity in the Canary region. *Geophysical Research Letters*, *35*(7). Doi: 10.1029/2008GL033329

Bindoff, N. L., & Mcdougall, T. J. (1994). Diagnosing Climate Change and Ocean Ventilation Using Hydrographic Data. *Journal of Physical Oceanography*, *24*(6), 1137-1152. Doi:10.1175/15200485(1994)024<1137:DCCAOV>2.0.CO;2

Bryden, H. L., Griffiths, M. J., Lavin, A. M., Millard, R. C., Parrilla, G., & Smethie, W. M. (1996). Decadal Changes in Water Mass Characteristics at 24°N in the Subtropical North Atlantic Ocean. *Journal of Climate*, *9*(12), 3162-3186. Doi: 10.1175/1520-0442(1996)009<3162:DCIWMC>2.0.CO;2

Casanova-Masjoan, M., Pérez-Hernández, M. D., Vélez-Belchí, P., Cana, L., & Hernández-Guerra, A. (2020). Variability of the Canary Current Diagnosed by Inverse Box Models. *Journal of Geophysical Research: Oceans*, *125*(8). Doi:10.1029/2020JC016199

Chidichimo, M. P., Kanzow, T., Cunningham, S. A., Johns, W. E., & Marotzke, J. (2010). The contribution of eastern-boundary density variations to the Atlantic meridional overturning circulation at 26.5° N. *Ocean Science*, *6*(2), 475-490. Doi:10.5194/os-6-475-2010

Cunningham, S. A., & Alderson, S. (2007). Transatlantic temperature and salinity changes at 24.5°N from 1957 to 2004. *Geophysical Research Letters*, *34*(14), L14606. Doi:10.1029/2007GL029821

Curry, R., & Mauritzen, C. (2005). Dilution of the Northern North Atlantic Ocean in Recent Decades. *Science*, *308*(5729), 1772-1774. Doi:10.1126/science.1109477

Fraile-Nuez, E., Machín, F., Vélez-Belchí, P., López-Laatzen, F., Borges, R., Benítez-Barrios, V., & Hernández-Guerra, A. (2010). Nine years of mass transport data in the eastern boundary of the North Atlantic Subtropical Gyre. *Journal of Geophysical Research*, *115*(C9), C09009. Doi:10.1029/2010JC006161

Fu, Y., Karstensen, J., & Brandt, P. (2017). A Atlantic Meridional Overturning Circulation at 14.5° N in 1989 and 2013 and 24.5° N in 1992 and 2015: volume, heat, and freshwater transports. *Ocean Science,* 14, 589-616. Doi:10.5194/os-14-589-2018

Fuglister, F. C. (1960). Atlantic Ocean atlas of temperature and salinity profiles and data from the International Geophysical Year of 1957-1958. Woods Hole Oceanographic Institution. Doi:10.1575/1912/4331

Harvey, J., & Arhan, M. (1988). The Water Masses of the Central North Atlantic in 1983—84. *Journal of Physical Oceanography*, *18*(12), 1855-1875. Doi: 10.1175/1520-0485(1988)018<1855:TWMOTC>2.0.CO;2

Hernández-Guerra, A., Espino-Falcón, E., Vélez-Belchí, P., Dolores Pérez-Hernández, M., Martínez-Marrero, A., & Cana, L. (2017). Recirculation of the Canary Current in fall 2014. *Journal of Marine Systems*, *174*, 25-39. Doi: 10.1016/j.jmarsys.2017.04.002

Hernández-Guerra, A., Pelegrí, J. L., Fraile-Nuez, E., Benítez-Barrios, V., Emelianov, M., Pérez-Hernández, M. D., & Vélez-Belchí, P. (2014). Meridional overturning transports at 7.5N and 24.5N in the Atlantic Ocean during 1992–93 and 2010–11. *Progress in Oceanography*, *128*, 98-114. Doi: 10.1016/j.pocean.2014.08.016

Hobday, A. J., Alexander, L. V., Perkins, S. E., Smale, D. A., Straub, S. C., Oliver, E. C. J., Benthuysen, J. A., Burrows, M. T., Donat, M. G., Feng, M., Holbrook, N. J., Moore, P. J., Scannell, H. A., Sen Gupta, A., & Wernberg, T. (2016). A hierarchical approach to defining marine heatwaves. *Progress in Oceanography*, *141*, 227-238. Doi: 10.1016/j.pocean.2015.12.014

Kanzow, T., Cunningham, S. A., Johns, W. E., Hirschi, J. J.-M., Marotzke, J., Baringer, M. O., Meinen, C. S., Chidichimo, M. P., Atkinson, C., Beal, L. M., Bryden, H. L., & Collins, J. (2010). Seasonal Variability of the Atlantic Meridional Overturning Circulation at 26.5°N. *Journal of Climate*, *23*(21), 5678-5698. Doi: 10.1175/2010JCLI3389.1

Knoll, M., Hernández-Guerra, A., Lenz, B., López Laatzen, F., Machín, F., Müller, T. J., & Siedler, G. (2002). The Eastern Boundary Current system between the Canary Islands and the African Coast. *Deep Sea Research Part II: Topical Studies in Oceanography*, *49*(17), 3427-3440. Doi: 10.1016/S0967-0645(02)00105-4

Liu, M., & Tanhua, T. (2021). Water masses in the Atlantic Ocean: Characteristics and distributions. *Ocean Science*, *17*(2), 463-486. Doi:10.5194/os-17-463-2021

Machín, F., Pelegrí, J. L., Fraile-Nuez, E., Vélez-Belchí, P., López-Laatzen, F., & Hernández-Guerra, A. (2010). Seasonal Flow Reversals of Intermediate Waters in the Canary Current System East of the Canary Islands. *Journal of Physical Oceanography*, *40*(8), 1902-1909. Doi: 10.1175/2010JPO4320.1

McNichol, A. P., Schneider, R. J., von Reden, K. F., Gagnon, A. R., Elder, K. L., Nosams, Key, R. M., & Quay, P. D. (2000). Ten years after – The WOCE AMS radiocarbon program. *Nuclear Instruments and Methods in Physics Research Section B: Beam*

Interactions with Materials and Atoms, *172*(1-4), 479-484. Doi: 10.1016/S0168-583X(00)00093-8

Navarro-Pérez, E., & Barton, E. D. (2001). Seasonal and interannual variability of the Canary Current. *Scientia Marina*, *65*(S1), 205-213. Doi:10.3989/scimar.2001.65s1205

Parrilla, G., Lavín, A., Bryden, H., García, M., & Millard, R. (1994). Rising temperatures in the subtropical North Atlantic Ocean over the past 35 years. *Nature*, *369*(6475), 48-51. Doi:10.1038/369048a0

Parrilla, G., Neuer, S., Traon, P.-Y. L., & Fernández, E. (2002). Topical Studies in Oceanography: Canary Islands Azores Gibraltar Observations (CANIGO). Vol. 2: studies of the Azores and Gibraltar regions. *Deep Sea Research Part II: Topical Studies in Oceanography*, *49*(19), 3951-3955. Doi: 10.1016/S0967-0645(02)00136-4

Pastor, M. V., Vélez-Belchí, P. and Hernández-Guerra, A. (2015). Water masses in the Canary Current Large Marine Ecosystem. In: *Oceanographic and biological features in the Canary Current Large Marine Ecosystem*. Valdés, L. and Déniz-González, I. (eds). IOC-UNESCO, Paris. IOC Technical Series, No. 115, pp. 73-79. URI: http://hdl.handle.net/1834/9178.

Pérez-Hernández, M. D., Hernández-Guerra, A., Fraile-Nuez, E., Comas-Rodríguez, I., Benítez-Barrios, V. M., Domínguez-Yanes, J. F., Vélez-Belchí, P., & De Armas, D. (2013). The source of the Canary current in fall 2009: The Source of the Canary Current. *Journal of Geophysical Research: Oceans*, *118*(6), 2874-2891. Doi: 10.1002/jgrc.20227

Pérez-Hernández, M. D., McCarthy, G. D., Vélez-Belchí, P., Smeed, D. A., Fraile-Nuez, E., & Hernández-Guerra, A. (2015). The Canary Basin contribution to the seasonal cycle of the Atlantic Meridional Overturning Circulation at 26°N. *Journal of Geophysical Research: Oceans*, *120*(11), 7237-7252. Doi: 10.1002/2015JC010969

Reißig, S., Nürnberg, D., Bahr, A., Poggemann, D. -W., & Hoffmann, J. (2019). Southward Displacement of the North Atlantic Subtropical Gyre Circulation System During North Atlantic Cold Spells. *Paleoceanography and Paleoclimatology*, 2018PA003376. Doi: 10.1029/2018PA003376

Roemmich, D., & Wunsch, C. (1985). Two transatlantic sections: Meridional circulation and heat flux in the subtropical North Atlantic Ocean. *Deep Sea Research Part A. Oceanographic Research Papers*, *32*(6), 619-664. Doi:10.1016/0198-0149(85)90070-6

Stramma, L., & Siedler, G. (1988). Seasonal changes in the North Atlantic subtropical gyre. *Journal of Geophysical Research*, *93*(C7), 8111. Doi: 10.1029/JC093iC07p08111

Tel, E., Balbin, R., Cabanas, J.-M., Garcia, M.-J., Garcia-Martinez, M. C., Gonzalez-Pola, C., Lavin, A., Lopez-Jurado, J.-L., Rodriguez, C., Ruiz-Villarreal, M., Sánchez-Leal, R. F., Vargas-Yáñez, M., & Vélez-Belchí, P. (2016). IEOOS: The Spanish Institute of Oceanography Observing System. *Ocean Science*, *12*(2), 345-353. Doi: 10.5194/os-12-345-2016

Trenberth, K. E., & Caron, J. M. (2001). Estimates of Meridional Atmosphere and Ocean Heat Transports. *Journal of Climate*, *14*(16), 3433-3443. Doi: 10.1175/1520-0442(2001)014<3433:EOMAAO>2.0.CO;2

Vargas-Yáñez, M., Parrilla, G., Lavín, A., Vélez-Belchí, P., & González-Pola, C. (2004). Temperature and salinity increase in the eastern North Atlantic along the 24.5°N in the last ten years: TEMPERATURE INCREASE ALONG 24.5°N. *Geophysical Research Letters*, *31*(6). Doi: 10.1029/2003GL019308

Vélez-Belchí, P., Caínzos, V., Romero, E., Casanova-Masjoan, M., Arumí-Planas, C., Santana-Toscano, D., González-Santana, A., Pérez-Hernández, M. D., & Hernández-Guerra, A. (2021). The Canary Intermediate Poleward Undercurrent: Not another Poleward Undercurrent in an Eastern Boundary Upwelling System. *Journal of Physical Oceanography*. Doi:10.1175/JPO-D-20-0130.1

Vélez-Belchí, P., González-Carballo, M., Pérez-Hernández, M. D. and Hernández-Guerra, A. (2015). Open ocean temperature and salinity trends in the Canary Current Large Marine Ecosystem. In: Oceanographic and biological features in the Canary Current Large Marine Ecosystem. Valdés, L. and Déniz-González, I. (eds). IOC-UNESCO, Paris. IOC Technical Series, No. 115, pp. 299-308. URI: http://hdl.handle.net/1834/9196.

Vélez-Belchí, P., Hernández-Guerra, A., Fraile-Nuez, E., & Benítez-Barrios, V. (2010). Changes in Temperature and Salinity Tendencies of the Upper Subtropical North Atlantic Ocean at 24.5°N. *Journal of Physical Oceanography*, *40*(11), 2546-2555. Doi: 10.1175/2010JPO4410.1

Vélez-Belchí, P., Pérez-Hernández, M. D., Casanova-Masjoan, M., Cana, L., & Hernández-Guerra, A. (2017). On the seasonal variability of the Canary Current and the Atlantic Meridional Overturning Circulation: SEASONALITY OF CANARY CURRENT AND AMOC. *Journal of Geophysical Research: Oceans*, *122*(6), 4518-4538. Doi: 10.1002/2017JC012774

Yu, J., Zhang, X., Li, L., Shi, C., & Ye, Y. (2020). Salient difference of sea surface temperature over the North Atlantic in the spring following three super El Niño events. *Environmental Research Letters*, *15*(9), 094040. Doi: 10.1088/1748-9326/aba20a